sciendo

Civil and Environmental Engineering
Vol. 19, Issue 1, 1-16, DOI: 10.2478/cee-2023-0001

STRUCTURAL BEHAVIOR OF GFRP - RC SLENDER COLUMNS UNDER VARIOUS ECCENTRICITY LOADING CONDITIONS

Rusul Z. HAMED[1,*], Hassan F. HASSAN[1]

[1] Department of Civil Engineering, Collage of Engineering, Mustansiriyah University, Baghdad, Iraq.
[*] corresponding author: rusulzuheir@gmail.com

Abstract

Glass fibers reinforced polymer (GFRP) were used to longitudinally and transversally 12 columns and while the other 4 columns were reinforced with steel or steel and GFRP as reference specimens. This research dealt with several parameters under different loading conditions, such as the reinforcing material and spacing between ties. This study aims to find out the ability of the reinforced columns with GFRP to bear the loads. In addition, investigate the mode of failure in these columns and their appropriateness in the structures since the columns are compression members. The tested results revealed that the concentric loading columns give higher resistance than their eccentrically loaded counterparts. Also, the hybrid column (steel and GFRP) had the highest peak load compared with the fully reinforced steel and GFRP columns. In addition, the fully GFRP RC- column had an ultimate load slightly less than its steel counterpart under the same loading condition.

Keywords:

GFRP;
Columns;
Concentric;
Eccentric;
Ductility.

1 Introduction

The concept of columns is vertical load-bearing components primarily carrying axial compressive loads, which are utilized to transfer the structure's load to the foundation. Beams, floors, and columns in reinforced concrete structures are constructed in a single piece. Over a portion of the cross-section, the bending motion of the column may provide tensile forces. Still, columns are referred to as compression members due to the fact that compressive loads dominate their behavior [1]. The presence of facilities in places with harsh climatic conditions in terms of moisture negatively affects the reinforcing steel, causing it to rust. And buildings exposed to the magnetic field, such as magnetic resonance rooms, reinforcing steel may play a negative role in the purpose of its construction furthermore the high price of steel relative to fibers and other reasons for introducing fibers in the reinforcement and enhancement of concrete structures as a good alternative to steel, so many studies have dealt with research in this field [2-4]. In the past two decades, the use of FRP bars for reinforcing structural concrete elements has expanded significantly. The majority of structural applications of FRP bars to date have been in flexural components where tensile stresses dominate structural behavior and failure [5, 6]. Nevertheless, it is not advised to use FRP as the primary reinforcement for compression members such as columns because of its insufficient compressive strength, as specified by ACI-440-1R [7]; however, it may be preferable to use FRP bars in the tension zone for eccentrically loaded columns where significant tensile stresses may arise. Prior studies have investigated that using GFRP bars as an alternative to steel bars in columns subjected to eccentric loads enhances the ultimate failure load [8, 9]. The utilization of (GFRP) bars in concrete columns is restricted to research, although its usage in concrete beams is more prevalent [10]. In contrast, FRP composites have a density between one-quarter and one-fifth that of steel, magnetic and electrical are non-conductivity, a reduced coverage needs, and a lower modulus of elasticity than steel bars [7]. Some of these investigations revealed that GFRP or CFRP transverse reinforcements improved confinement of the concrete core and boosted deformation capabilities [11, 12].

Tobbi et al. [13] tested the mechanical performance of FRP-reinforced concrete columns exposed to concentrically applied loads. The arrangement of transverse reinforcement, reinforcement type (GFRP or steel bars), tie spacing, compressive strength, reinforcement ratio, and confining volumetric stiffness were investigated. Twenty RC column specimens with a 350 x 350 mm square cross-section and 1400 mm length were subjected to a concentric force applied. Nineteen of the specimens are reinforced with FRP and steel bars based on various specifications, while one column is plane concrete (without reinforcement). Results indicate that FRP reinforcement is superior to steel reinforcement for decreasing final axial strain.

Alwash et al. [14] experimented on the behavior of short CFRP RC columns under eccentric loading. Fourteen models with a cross-section of 140 x 140 mm and an overall height of 820 mm were examined in the experimental test. The distance between the middle corbels is 400 mm. Three of these models, one without reinforcement and two with steel reinforcement, served as control specimens, while eleven columns were reinforced with CFRP bars. The research evaluated the effects of compressive strength, eccentricity ratio, and longitudinal reinforcement. It has been determined that columns reinforced with CFRP bars increase the ultimate load by 38.21 % under load eccentricity ratio e/h = 0.857 and reduce the ultimate load by 3.78 % under axial load when compared to columns reinforced with steel bars.

Othman et al. [15] conducted an experimental investigation on eighteen RC columns with cross-section dimensions of 150 x 150 mm and a total length of 1500 mm exposed to eccentric axial loads. Three columns were reinforced with steel bars and ties as reference specimens, whereas fifteen were reinforced with CFRP bars and ties. Each group consisted of three columns with similar reinforcing features but was evaluated under various eccentricity circumstances e = 0 mm, 75 mm, and 150 mm. The amount of eccentricity influences the failure mechanism and behavior of CFRP RC columns, according to the findings. Reducing tie spacing has negligible influence on the axial capacity of concentrically loaded columns. For columns exposed to eccentric load, however, reducing tie spacing decreases axial ability by about 12.4 percent for a 150 mm e/h = 0.1 column with eccentricity. Moreover, under eccentric load, all CFRP RC columns collapsed due to concrete crushing on the compression side, and the highest tensile strain in the longitudinal bars did not exceed 34 % of the ultimate tensile strain of the bar.

El-Gamal et al. [16] examine nine 230 mm diameter and 1500 mm high low-strength circular concrete columns reinforced with GFRP bars and spirals under axial stress. The parameters of the tests comprised the kind of reinforcement (GFRP or steel), the longitudinal reinforcement ratio, and the spiral spacing. The GFRP-RC columns were found to behave the same way as their steel-RC counterparts in tests. The GFRP-RC columns, on the other hand, had a lower initial peak load than their steel-reinforced counterparts. The columns' capacity was marginally increased by increasing the GFRP reinforcement ratios. The second peak load of the highly confined columns was much higher and demonstrated superior tensile failure in the highly confined columns. The findings demonstrated that the Canadian Standard Association calculation was too cautious for columns with high reinforcement ratios. Three different confinement models were utilized for the maximum confined concrete strength, and they could estimate it relatively reasonably. The load-axial displacement of the tested columns was also predicted using an existing analytical model, which showed acceptable agreement with the experimental results up to the first peak loads. Post-peak, on the other hand, there were significant departures.

Al-Helfi and Alami [17] investigate the strengthened column by steel-fiber-reinforced (SFR) and (CFRP) on a portion of the entire length of the column under axial force to determine the effective length responsible for the increase in the column's resistance to buckling. Seven specimens were developed as slender reinforced columns with 120 x 60 mm in cross-section and 2000 mm in length. It was shown that reinforcing the middle half of the column length with SFR yielded the same ultimate load as strengthening the whole column with the same material. In addition, it was discovered that the SFR-reinforced column raised its ultimate load by 42.6 %, 42.1 %, and 33.3 % for strengthened lengths of L, $L/2$, and $L/3$, respectively, compared to the non-reinforced column. The interaction diagram for the column strengthened with CFRP is larger than the interaction diagram for the column reinforced with SFR, which is larger than the interaction diagram for the unreinforced column.

2 Research significance

This work included an experimental investigation of the behavior of concrete slender columns reinforced with fully GFRP bars under concentric and eccentric loads. Its objective was to assess the

influence of GFRP bars as longitudinal and transverse reinforcement on the performance of concrete column members, with a particular emphasis on the strength and strain capacity of RC components. The failure process is explained, also the effect clarification of various longitudinal reinforcement ratios and different spacing between ties on the slender RC-columns performance. The purpose of the work was also to highlight the consequences of the cover spalling process.

3 Experimental program

3.1 Tested columns description

Sixteen reinforced concrete columns with cross-section dimensions of 140 x 140 mm and a height of 1200 mm with an effective length of 1000 mm were examined. Fig.1 shows the dimension of the specimen. Four of the 16 RC-columns were reinforced with steel and served as reference columns. However, the other specimens were fully reinforced with GFRP. Two sets of columns were formed, including a different reinforcement ratio. The first one with a reinforcement ratio of 1.6 %, equivalent to four bars with a diameter of 10 mm, and the other with a reinforcement ratio of 4.1 %, equal to four bars of 16 mm. Each group consists of three columns that have been subjected to varying concentric and eccentric loads at 0, 30, and 60 mm from the center line. Furthermore, ties with a diameter of 6 mm were utilized to distribute reinforcement transversely across (stirrups) the bars at 60 and 120 mm intervals. The specimens have been identified depending on the longitudinal bar reinforcing material (steel or GFRP) and its diameter, transverse reinforcement material, and tie spacing, in addition to applied load eccentricity. As an example, specimen G10-TG60-E30. Table 1 lists data from the experimental program.

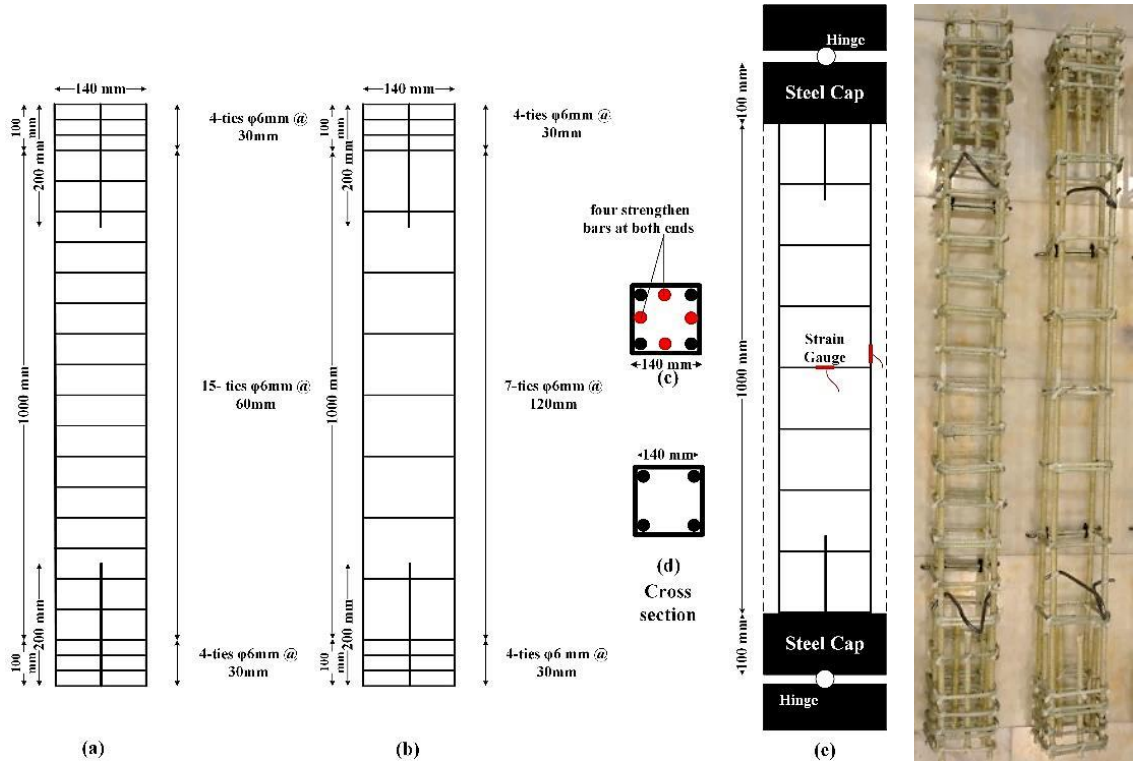

Fig. 1: Specimen's dimension: a), b), c), d) reinforcement details of the columns and their cross-section, e) RC-Column with steel cap connection, f) cages of columns.

Table 1: Data of the experimental program.

Col. ID	Rein. ratio [%]	Longitudinal reinforcement		Transverse reinforcement		Eccentricity [mm]	*e*/*h* [%]
		Type	Diameter [mm]	Type	Spacing [mm]		
G10-TG60-E0	1.6	GFRP	10	GFRP	60	0	0
G10-TG60-E30	1.6	GFRP	10	GFRP	60	30	21.2
G10-TG60-E60	1.6	GFRP	10	GFRP	60	60	42.86
G10-TG120-E0	1.6	GFRP	10	GFRP	120	0	0
G10-TG120-E30	1.6	GFRP	10	GFRP	120	30	21.2
G10-TG120-E60	1.6	GFRP	10	GFRP	120	60	42.86
G16-TG60-E0	4.1	GFRP	16	GFRP	60	0	0
G16-TG60-E30	4.1	GFRP	16	GFRP	60	30	21.2
G16-TG60-E60	4.1	GFRP	16	GFRP	60	60	42.86
G16-TG120-E0	4.1	GFRP	16	GFRP	120	0	0
G16-TG120-E30	4.1	GFRP	16	GFRP	120	30	21.2
G16-TG120-E60	4.1	GFRP	16	GFRP	120	60	42.86
S10-TG120-E60	1.6	Steel	10	GFRP	120	60	42.86
S10-TS120-E60	1.6	Steel	10	steel	120	60	42.86
S16-TG120-E60	4.1	Steel	16	GFRP	120	60	42.86
S16-TS120-E60	4.1	Steel	16	Steel	120	60	42.86

It is worth mentioning that the ties were intensified at the two ends by 100 mm for each end of each column to strengthen these regions by reducing their spacing to 30 mm. For the same purpose, extra 200 mm long bars with the same diameter as the longitudinal bars were placed between the main reinforcing bars in the relevant part to increase the column's resistance to eccentric loads, with an average of additional four bars at each end see Fig. 2.

a) b) c)

Fig. 2: Column reinforcement cage: a) reinforcement ratio 1.6 %, b) reinforcement ratio 4.1 %, c) reinforcement cage of reference column.

Two strain gauges were installed in the mid-height at the tension side of the cage as this is the most probable zone of failure. All the strain gages were wired in a quarter-bridge to measure the strain developed at the longitudinal and transverse reinforcement. In the longitudinal and transverse reinforcements, one was used to measure longitudinal strain and was attached to the longitudinal bar; the other was used to measure transverse strain and attached to the transverse reinforcement. To ensure that the applied loads are distributed uniformly and to minimize unintended local failures in the loading zones, all columns were confined with top and bottom rigid steel caps to raise the amount of confining in these stress concentration regions. Steel caps were provided with adjustable steel hinge bearings to achieve the specified eccentricity and to imitate the situation of a perfect pin-ended column Fig. 3 shows a steel cape and hinges (the supports).

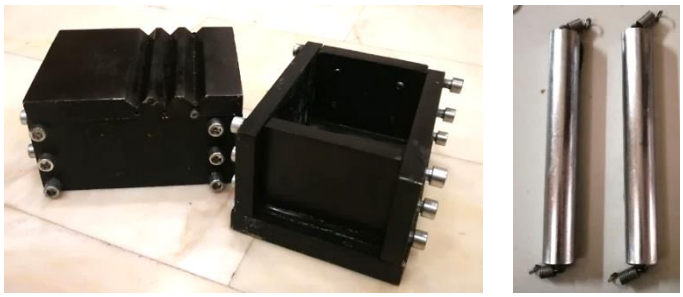

a) b)

Fig. 3: a) steel cape, b) steel hinge.

3.2 Material

All columns were made from ready-mixed concrete with a typical compressive strength of 22.15 MPa on average. The compressive strength of concrete was determined following ASTM C39 [18] using 150 x 300 mm standard cylinders. The GFRP producer company evaluated the GFRP bars in accordance with ASTM D7205 [19] and provided the author with the following information: the tensile strength of 896, 827, 724 MPa for 6, 10, and 16 mm bar diameter respectively, and the elastic modulus was 46 GPa.

3.3 Instrumentation and test setup

Two LVDTs (Linear Variable Displacement Transducers) were used to detect longitudinal and transverse displacement; they were attached vertically and laterally at the mid-height of the column shaft by the magnetic base. The LVDTs used are with an accuracy of 0.01 mm and linearity of up to 0.075 %, insensitive to shock and vibration. It was calibrated following the data logger user's manual procedure for the LVDT connected part. However, the calibration was performed by applying known movement and measuring the corresponding reading. Fig. 4 shows the magnetic base and LVDTS.

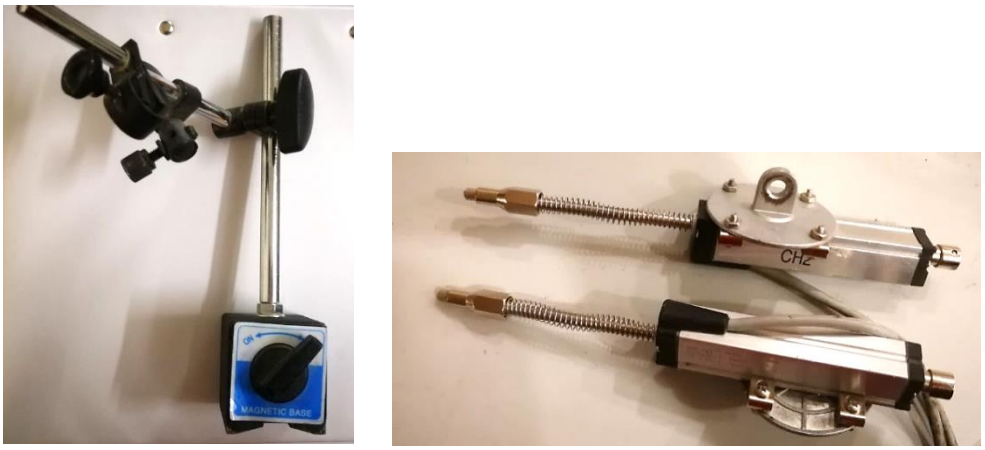

a) b)

Fig. 4: a) magnetic base, b) LVDT.

The load cell depicted in Fig. 5 was used to measure the compression load of the specimen subjected to press forces by means of the electric compressive machine. The load cell used was constructed from stainless steel with a capacity of 1000 kN shows the load cell.

The main principles of data acquisition are sampling signals that measure and reflect the actual physical conditions and convert the obtained signals into numerical values that a computer can process. The data logger used in this study was locally assembled with a capacity of 5 channels compatible with load cells, LVDTs, and strain gauges. Datalogger is connected directly to the computer. Readings are taken at one reading per second. The data is automatically stored in memory and downloaded to the computer in real-time for simultaneous monitoring of the test being conducted. This version is compatible with a full range of transducers for different test requirements. See Fig. 6. It is worth mentioning, that the front of the column's face is dotted, indeed this is for further advanced particle image velocimetry (PIV) analysis which is out of the scope of the present paper.

Fig. 5: The load cell.

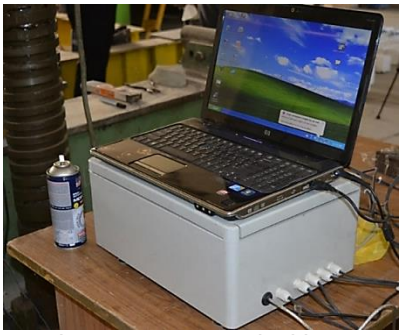

Fig. 6: Data logger connected with computer PC.

4 Experimental results and discussion

4.1 Ultimate load and failure mode

All the columns were tested until failure occurred. The failure modes rely on the kind of reinforcement (the material used in the reinforcement) and the type of loading (concentric or eccentric). For the specimens examined under concentric loading, capillary cracks (scattered cracks) appeared with about 90 % of the ultimate applied load, as the rate of axial loading increases, cracks progress, causing concrete cover spalling. Afterward, cracks were created in the concrete core, which led to the expansion of the core, and consequently, lateral pressure was produced on the transverse reinforcement.

In general, the failure in the specimens exposed to the concentric load, which was made of GFRP, started with a crack in the concrete cover, followed by buckling and rupture in the longitudinal and transverse reinforcement then spalling in the concrete core appeared cracks in the tension side prior to crushing of the concrete cover in the compression region, which reached about 85 % of the peak load, followed by a buckling of the longitudinal reinforcement with respect to the steel bar and fracturing in relation to the GFRP. Also, rupture in GFRP ties due to dilation in concrete core caused by progressing in the applied load. Fig. 7 represents the failure mode of specimens under eccentric loads. The specimens which ready for testing were divided according to the type of reinforcement ratio, the material of reinforcement, and eccentricity ratios, according to Table 2 shown below.

Table 2: Groups of testing specimens and their characteristics.

Col. ID	Rein [%]	Long. diam. [mm]	S_{ties}	*e/h*	*Pu* [kN]	L. Rein. STR. [%]	T. Rein. STR. [%]	δ_y	δ_L	P_{bars}	P_{bars}/P_u [%]	*DI*
G10-TG60-E0	1.6	10	60	0	278.76	0.0732	0.962	1.535	0.04	10.58	3.79	1.738
G10-TG120-E0			120		269	-0.0096	0.274	2.52	0.01	1.388	0.515	3.31
G10-TG60-E30			60	0.21	137.34	0.028	0.030	2.27	2.91	-	-	1.56
G10-TG120-E30			120		193.257	0.006	0.183	5.04	2.4	-	-	1.65
G10-TG60-E60			60	0.42	69.651	0.122	0.096	3.85	5.35	-	-	1.48
G10-TG120-E60			120		65.727	0.0084	0.756	2.99	16.24	1.214	1.84	2.47
G16-TG60-E0	4.1	16	60	0	311	-0.0948	1.19	1.06	0.028	35.04	11.266	1.8
G16-TG120-E0			120		301.22	-0.042	0.14	2.29	0.01	15.52	5.15	2.47
G16-TG60-E30	4.1	16	60	0.21	252.117	0.14	0.065	3.26	3.01	-	-	1.03
G16-TG120-E30			120		287.433	0.036	0.084	3.19	1.96	-	-	1.067
G16-TG60-E60			60	0.42	193.257	0.006	0.0183	6.08	2.4	-	-	1.22
G16-TG120-E60			120		106.929	0.0144	-0.022	4.92	1.43	5.33	4.98	1.5
S10-TG120-E60	1.6	10	120	0.42	143.22	0.0165	-	5.78	6.24	10.43	7.282	1.48
S10-TS120-E60					68.67	0.0049	-	1.46	3.19	3.091	4.50	1.31
S16-TG120-E60	4.1	16	120	0.42	200.124	0.0138	0.252	3.91	3.33	22.197	11.09	2.44
S16-TS120-E60					122.652	0.0116	0.98	4.73	7.46	18.72	15.09	1.08

Rein % Longitudinal reinforcement ratio. (Long.Diam.mm) Bar's diameter. S_{ties} spacing between ties. *Pu* ultimate load. δ*V* vertical displacement. δ*L* Lateral displacement. *DI* ductility index.

a) G10-G60-E0 b) G10-TG120-E0 c) G16-TG60-E0 d) G16-TG120-E0

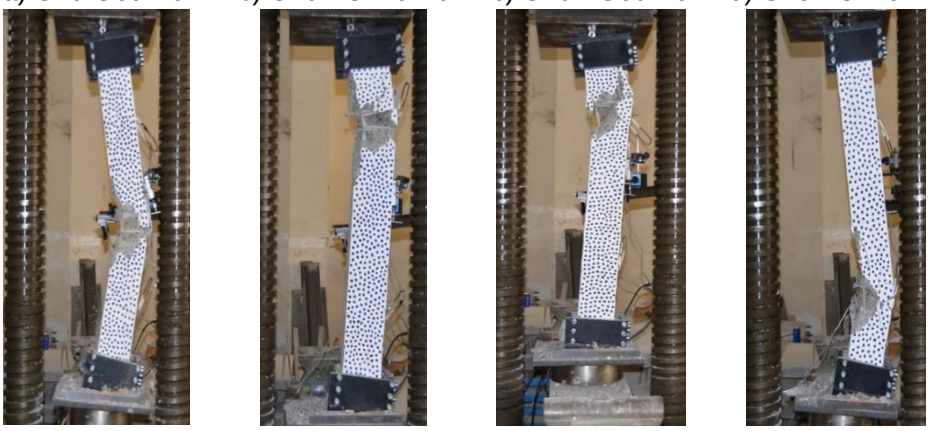

e) G10-TG60-30 f) G10-TG60-E60 g) G10-TG120-30 h) G10-TG120-60

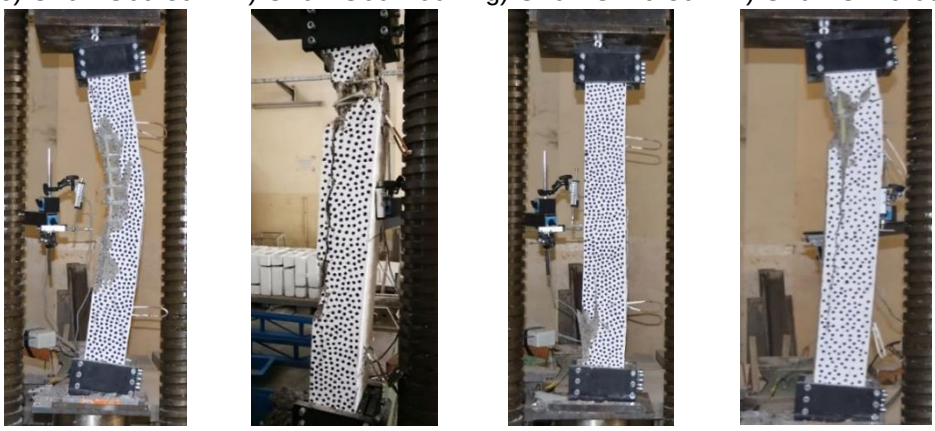

i) G16-TG60-E30 j) G16-TG60-E60 k) G16-TG120-E30 l) G16-TG120-E60

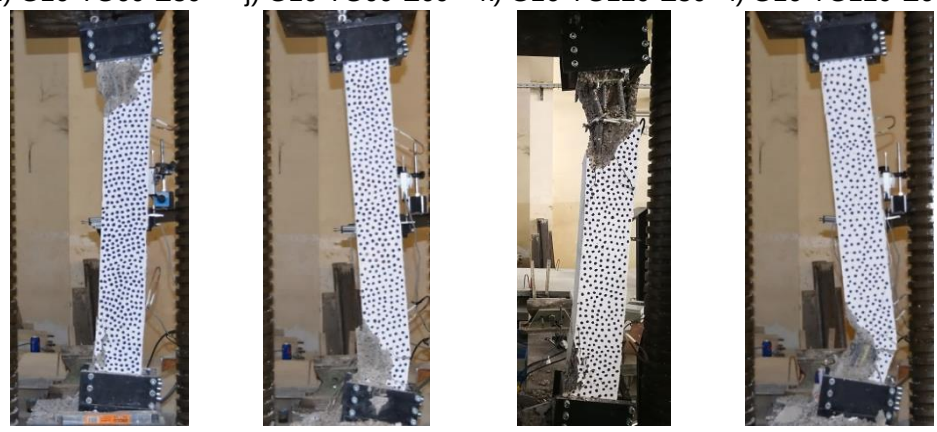

m) S10-TG120-E60 n) S10-TS120-E60 o) S16-TG120-60 p) S16-TS120-E60

Fig. 7: Mode of failure for specimens.

4.2 Longitudinal and transverse reinforcement strain response

Curves of ultimate load versus longitudinal reinforcement strain for both reinforcement ratios are illustrated in Fig. 8. It can be noted from Table 2 that the column bearing increases when increasing the reinforcement ratio, and thus the strain in the longitudinal reinforcement increases. As a result, the increasing ratio was 4.687 % is a margin ratio, and 77.78 % for the G16-TG60-E0 and G16-TG120-E0 columns, respectively. As for 30 mm eccentricity loading was 31.43 % and 66 % for columns G10-TG60-E30 and G10-TG120-E30 respectively. Finally, the growth rate was 85.29 % and 17.14 % for columns G10-TG60-E60 and G10-TG120-E60, respectively, for 60 mm eccentricity loading, relative to the lowest load level.

It is noticed through the analysis of the results in the case of concentric loading that the columns with the highest reinforcement ratio have the highest strain value due to the high endurance value. In contrast, when exposed to the eccentric loading of 30 and 60 mm, it was found that the columns with the lowest reinforcement ratio had the highest amount of strain. This reason can be attributed to the fact that the columns under eccentric loading are subjected to two types of stresses, axial load and moment generated due to the eccentricity, which causes an increase in the columns' strain with a lower reinforcement ratio.

On the other hand, it can be noted from Table 2 that the column bearing capacity in the concentric loading increases when reducing the confinement, and thus the strain in the longitudinal reinforcement increases. So, the increasing proportion was 85.71 %, and 55.13 % for the G10-TG60-E0 and G16-TG60-E0 columns, respectively when concentrically loading. At 30 mm eccentricity loading the column resistance increases when the spacing between ties increases, but the ultimate longitudinal reinforcement strain decreases so, the growth rate was 57.14 % and 71.42 % for columns G10-TG60-E30 and G16-TG60-E30, respectively. As for 60 mm eccentricity, the growth rate was 91.76 % and 33.3 % for columns G10-TG60-E60 and G16-TG60-E60, respectively as compared with the lowest load level. The results presented above found that reducing the tie spacing enhances the longitudinal reinforcement strain more than its counterpart with the higher spacing. It could be due to the confining efficiency provided by the high ratio of transverse reinforcement ratio.

The ultimate load versus longitudinal reinforcement strain is depicted in Fig. 8d for hybrid and fully (steel, GFRP) reinforcement under 60 mm eccentricity loading columns. As can be seen, all curves slop ascended linearly with the load progressing until reaching the peak of bearing capacity, followed by descending in slop until the failure occurred. The investigating data are listed in Table 2; the resistance in the hybrid column was higher than its two counterparts, then the fully steel-reinforced column, followed by the fully fiber-reinforced column for the two groups with 1.6 % and 4.1 % reinforcement ratios. But the values of longitudinal reinforcement strain for the 1.6 % reinforcement ratio group were in sequence from the highest to the lowest according to the load-bearing columns. In contrast, for columns of a group with a 4.1 % reinforcement ratio, the GFRP-reinforced column recorded the highest strain value, followed by the fully reinforced with steel, and then the hybrid column. The reduction in strain was 45.71 % and 48.57 % for columns S10-TS120-E60 and S10-TG120-E60, respectively. Also, 39.167 % and 65.83 % for columns S16-TS120-E60 and S16-TG120-E60. Relative to the lowest load level. It is clear from these results that the column fully reinforced with GFRP had the highest strain than full steel and hybrid columns under the same load level; this is since the ultimate strain for GFRP is 2.4 - 3.6 %, while 0.12 - 0.2 % for steel.

While curves of ultimate load versus transverse reinforcement strain for both reinforcement ratios are depicted in Fig. 9. In addition, the experimental results are listed in Table 2. It can be seen that the column resistance increases when reducing the spacing between ties when loading was concentrically, and thus the transverse reinforcement strain increases. So, the rate of growth was 66.74 % and 88.03 % for the G10-TG60-E0 and G16-TG60-E0 columns, respectively.

Otherwise, the column resistance increases when increasing the spacing between ties for 30 and 60 mm eccentricity loads, and thus the transverse reinforcement strain increases. Where the rate of growth was 55.88 % and 14.5 % for the G10-TG120-E30 and G16-TG120-E30 columns, respectively. And was 89.94 % and 69.43 % for columns G10-TG120-E60 and G16-TG120-E60, respectively, concerning the lowest load. This discussion found that, in general, in concentric loading columns, reducing the spacing between ties enhances the resistance of columns thus, the strain in the stirrups increases due to the applied load. In contrast, in the eccentrically loaded column, the increased spacing between ties increases the bearing capacity of the column, so the transverse reinforcement strain rises.

Fig. 9d shows the relationship between longitudinal and transverse reinforcement strain values for the hybrid and fully (steel, GFRP) reinforced columns for the reinforcement ratios of 1.6 % and 4.1 %. The slope of the columns was linear and continued to rise with the loading rate increasing until the highest loading was reached. Table 2 shows the ties strain values for the hybrid and fully (steel, GFRP) reinforced columns for the Reinforcement ratios of 1.6 % and 4.1 %. There were missing data in Columns of Group with a reinforcement ratio of 1.6 %; perhaps an error occurred in installing the strain slice or in casting the models. For this reason, the transverse reinforcement strain has not recorded the readings of these columns. As for the group of columns with reinforcement of 4.1 %, the percentage decrease was 96.97 % and 90.91 % for columns G16-TG120-E60 and S16-TG120-E60, concerning the lowest load.

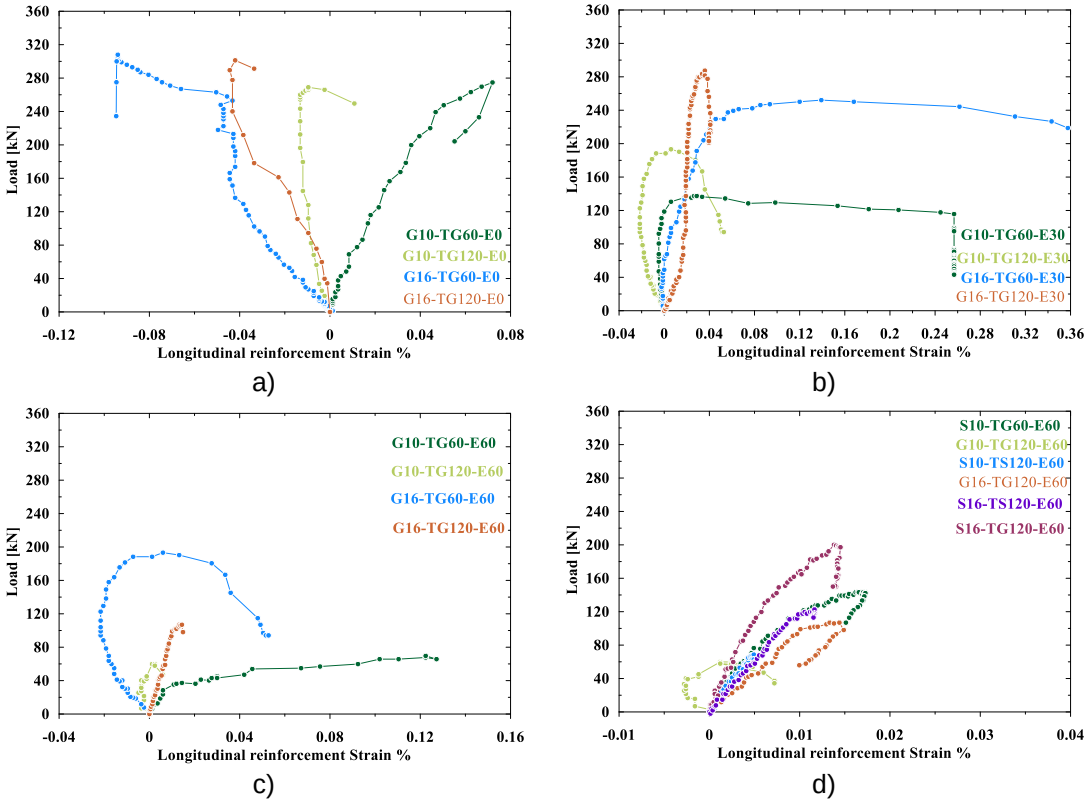

Fig. 8: Load-longitudinal reinforcement strain curves: a), b), c), d) for eccentricity 0, 30, 60 mm, hybrid and full (steel, GFRP) columns, respectively.

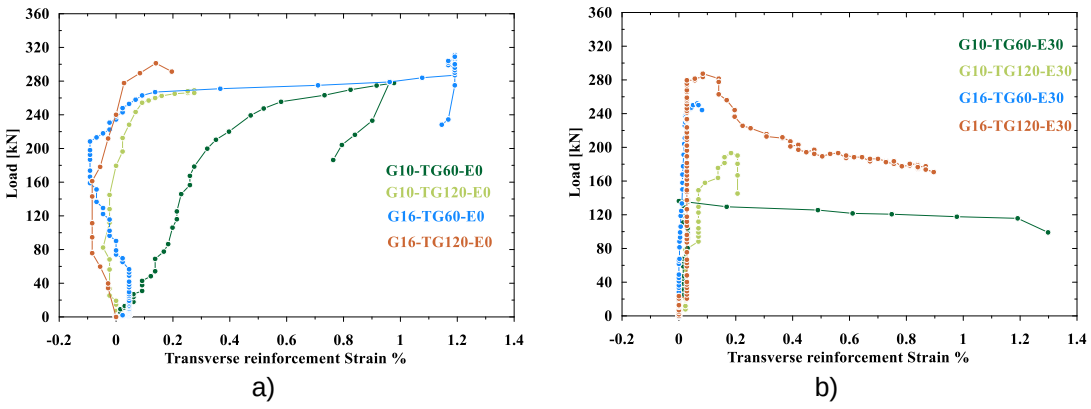

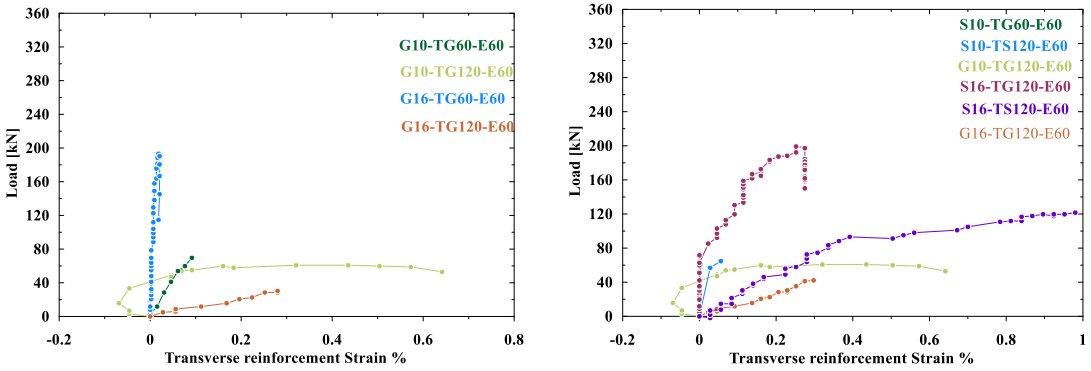

c) d)

Fig. 9: Load-transverse reinforcement strain curves: a), b), c), d) for eccentricity 0, 30, 60 mm, hybrid and full (steel, GFRP) columns, respectively.

4.3 Displacement response

Fig. 10 shows the relationship between ultimate load versus lateral displacement. As can be seen, there is a slight increasing displacement associated with progressing load until reaching the ultimate load, followed by failure. Inserted the test data in Table 2. It appeared that the column's bearing capacity increases when increasing the reinforcement ratio, and thus the lateral displacement decreases. So, the increasing proportion in concentric loading was 55.5 % for the G10-TG60-E0. On the other hand, there is the same displacement reading at the same load level for the G10-TG120-E0 and G16-TG120-E60 columns.

The growth rate for 30 mm eccentricity load was 84.2 % and 84.2 % for columns G10-TG60-E30 and G10-TG120-E30, respectively. Moreover, the increasing proportion for columns under 60 mm eccentricity loading was 96.82 % and 97.8 % for columns G10-TG60-E60 and G10-TG120-E60, respectively, compared with the lowest load level.

Evidently, from the previous discussions, increasing the reinforcement ratio enhances the ability of the columns to bear the loads imposed on them, which gives immunity against possible deformations. Thus, the displacement amount is reduced in columns with a higher reinforcement ratio than their counterparts with a lower reinforcement ratio.

On the other hand, it can also be noted that reducing the confinement spacing leads to increasing the columns' bearing capacity with concentric loading columns; hence, the lateral displacement decreases. So, the increasing proportion was 99.81 % and 98.46 % for the specimens G10-TG120-E0 and G16-TG120-E0, respectively. Also, for loading at 30 mm eccentricity, in sequence, the increment percentage was 69.41 % and 67.8 % for the G10-TG60-E30 and G16-TG60-E30 columns. Additionally, the increasing proportion for 60 mm eccentricity loading was 76.35 % and 62.93 % for the specimens G10-TG120-E60 and G16-TG120-E0, respectively, according to the minimum load level.

From these discussions, it was found that reducing the spacing between ties when applying concentric load on the specimens provides high confinement of the core, leading to enhancing the resistance of the shaft to the applied load thus, the lateral displacement is reduced. But the opposite result was found that when subjected to 30 mm eccentric loading, the increased tie spacing promotes the ability of the shaft to resist the applied load, thus decreasing the lateral displacement. As for the high eccentricity, found reverse behavior of 30 mm eccentric loading, the lateral displacement increased with increased tie spacing because of the higher bearing capacity.

The ultimate load versus lateral displacement is depicted in Fig. 10.d for hybrid and fully (steel, GFRP) reinforced columns under 60mm eccentricity loading. As indicated, all curves slop ascended linearly with the load progressing until reaching the peak of bearing capacity, followed by descending in slop until the failure occurred. The investigation results are listed in Table 2. It appeared the reduction percentage relative to the lowest load level was 85.52 % and 95.69 % for S10-TS120-E60 and S10-TG120-E60 columns, also 59.02 % and 97.13 % for specimens G16-TG120-E60 and S16-TG120-E60, respectively. It was found from this behavior that column G10-TG120-E60 had the highest lateral displacement. The reason could be that the fully GFRP reinforced column is the least bearing resistance for columns with a reinforcement ratio of 1.6 %. As for the columns with a reinforcement ratio of 4.1 %, the column S16-TS120-E60 had the most significant lateral displacement; this behavior may be attributed to the difference in size between the core of columns reinforced with full steel to their

counterparts reinforced transversely with GFRP. Where the concrete cover is 1.5, and 2.5 cm for GFRP and steel (according to ACI-code [2]) RC columns respectively.

Fig.11 shows the relationship between ultimate loads with vertical displacement. As can be seen, there is a linear ascending slope of increasing displacement associated with progressing load until reaching the ultimate load, followed by failure for all curves; Inserted the test data in Table 2. It appeared that column G10-TG60-E0 has a higher vertical displacement than G16-TG60-E0 by 51.8 %, whereas column G10-TG120-E0 has 32.53 % higher than G16-TG120-E0. Column G16-TG60-E30 has a higher displacement than G10-TG60-E30 by 8.09 %; it could be considered a margin value. In contrast, column G10-TG120-E30 has 48.61 % higher than G16-TG120-E30. Column G10-TG60-E60 has a higher displacement than G16-TG60-E60 by 46.36 %. Furthermore, column G10-TG120-E60 has 12.04 % higher than G16-TG120-E60.

From the previous discussion, it is found that the vertical displacement decreases by increasing the reinforcement ratio depending on high resistance.

Also, from the experimental result, it appears that when reducing confinement spacing increases the resistance of the concentric loading column, the vertical displacement will decrease. As a result, the increment was 43.05 % and 60.7 for specimens G10-TG120-E0 and G16-TG120-E0, respectively. While at 30 mm eccentricity loading Column G10-TG120-E30 has a higher displacement than G10-TG60-E30 by 46 %. On the contrary, column G16-TG60-E30 has 12.88 % higher than G16-TG120-E30. Finally, the increasing proportion was 8.5 % and 4.05 % for specimens G10-TG60-E60 and G16-TG120-E60, respectively, which could be considered margin values. All comparisons were with the minimal load level.

The ultimate load versus vertical displacement is depicted in Fig.11.d for hybrid and fully (steel, GFRP) RC columns under 60 mm eccentricity loading. As indicated, all curves slop ascended linearly with the load progressing until reaching the peak of bearing capacity, followed by descending in slop until the failure occurred. The investigation results are listed in Table 2; the reduction percentage relative to the lowest load was 59.53 % and 29.43 % for S10-TS120-E60 and S10-TG120-E60 columns and was 15.24 % and 71.54 % for specimens S16-TS120-E60 and S16-TG120-E60, respectively. Relative to the lowest carrying capacity. It found that columns reinforcing with fully GFRP have the highest vertical displacement because of their lowest bearing capacity. This is likely due to the steel's modulus of elasticity being higher than GFRP.

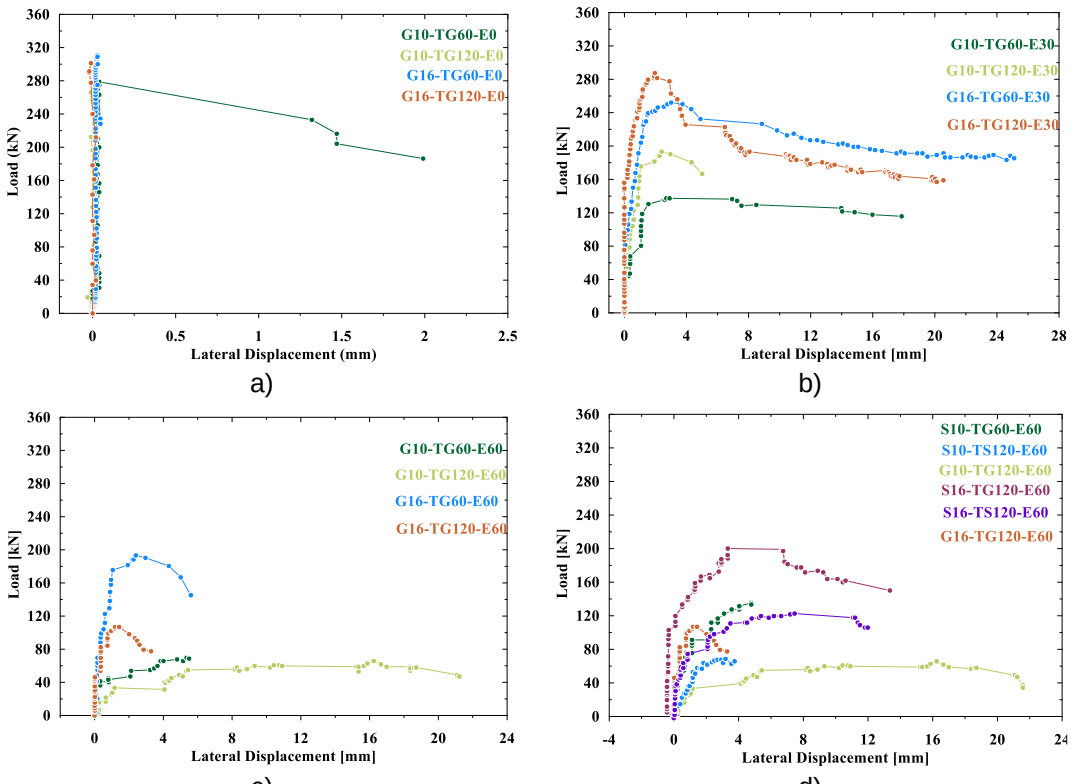

Fig. 10: Load-lateral displacement curves: a), b), c), d) for eccentricity 0, 30, 60 mm, hybrid and full (steel, GFRP) columns, respectively.

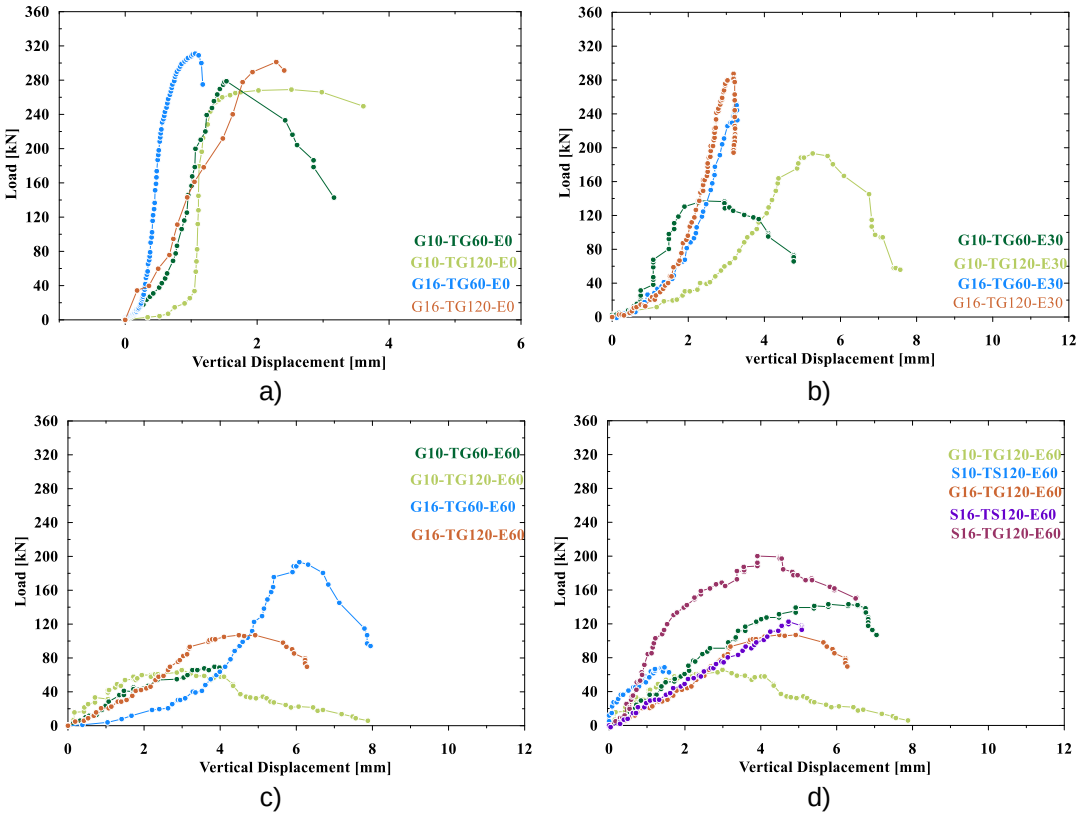

Fig. 11: Load-vertical displacement curves: a), b), c), d) for eccentricity 0, 30, 60 mm, hybrid and full (steel, GFRP) columns, respectively**.**

4.4 Ductility index

The ductility index, $DI = \delta_u/\delta_y$, for all columns can be determined as the ratio of the ultimate displacement δ_u to the yield displacement δ_y as suggested by Pessiki and Pieroni [20] and Elmesalami 2020 [21]. The ultimate displacement was calculated as the displacement observed at 85 % of the ultimate load in the descending part of the load-displacement relationship. The yield displacement, which is the vertical displacement obtained at the yield load, was found by extending the initial linear part of the load-displacement curve to intersect with a horizontal line corresponding to the peak load of the column. The determination method of the ductility index can be seen in Fig. 12.

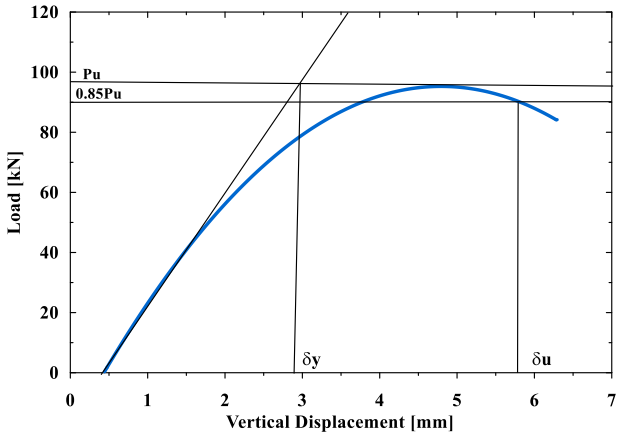

Fig. 12: Determination method of the ductility index [20, 21].

Fig. 13 shows the ductility index of fully GFRP-reinforced concrete columns with all different loading conditions adopted in this research. Each group of columns represents the reinforcement and eccentricity ratios of the columns. It was found that increasing the spacing between ties from 60 to 120

mm leads to increased ductility by specific amounts shown in Table 2. It is worth mentioning that the obtained results are consistent with Almessalami 2020 works [21].

It is evident that the DI of columns with 60 mm tie (stirrups) spacing decreased as the eccentricity increased. On the other hand, The DI values of columns of 120 mm tie (stirrups) spacing decrease when e/h is equal to 21 % and then increase when e/h reaches 42.85 %. This may be attributed to the reason that in concentrically loaded columns, the axial loads remain within the kern area of the column. However, it is displaced as the eccentricity increase, causing nonuniform stress distribution in the cross-section area, which accelerates the failure of eccentrically loaded columns.

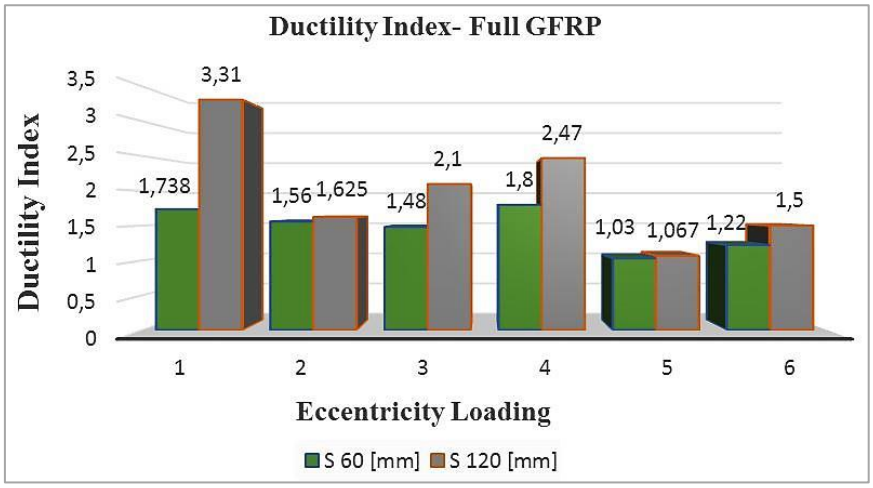

Fig. 13: Ductility index for full GFRP concrete columns: 1 - ρ 1.6 % E0, 2 - ρ 1.6 % E30, 3 - ρ 1.6 % E60, 4 - ρ 4.1 % E0, 5 - ρ 4.1 % E30, 6 - ρ 4.1 % E60.

Fig.14 illustrates the ductility index for groups 1 and 2, which refers to the reinforcement ratio of 1.6 % and 4.1 %, respectively for fully (steel, GFRP) reinforced columns. As depicted, it was found that reducing the spacing of 60 mm for columns reinforced with fully GFRP exhibited higher ductility than their counterpart which fully steel reinforced columns at 120 mm spacing between ties, for the two groups above by 12.98 and 12.96 %. The same observations were found by Almessalami 2020 [21].

This finding indicates that utilizing GFRP in reinforcing concrete columns by reducing confined spacing gives credit for GFRP to achieve the desired purpose of replacing steel, which is one of the aims of the current study.

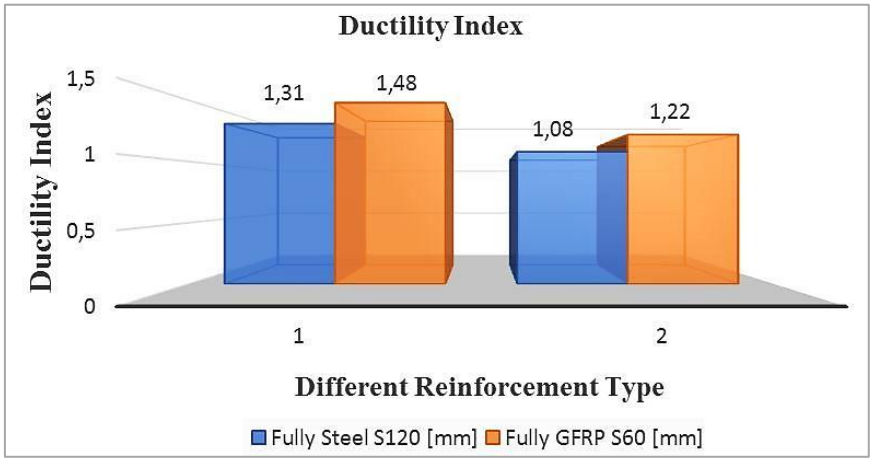

Fig. 14: Ductility index for fully (steel, GFRP) concrete columns at the different spacing between ties: 1 - ρ 1.6 %, 2 - ρ 4.1 %.

The ductility index of fully reinforced hybrid concrete columns and full (steel, GFRP) columns are represented in Fig.15. As it is clear that the column G10-TG120-E60 had the highest ductility. The increase with respect to the lowest ductility value is 12.98 % and 88.55 % for columns S10-TG120-E60 and G10-TG120-E60, respectively; which depicted a group (1) with a reinforcement ratio of 1.6 %.

While in a group (2) with a reinforcement ratio of 4.1 %, hybrid column S16-TG120-E30 was dominant, which has the highest ductility index with an increment of 125.93 % and 38.89 % for columns S16-TG120-E60 and G16-TG120-E60, in sequence. This result can be attributed to the fact that at the minimal reinforcement ratio, the effectiveness of steel did not appear in the columns' ductility clearly due to the low reinforcement ratio. On the other hand, when the reinforcement ratio was increased to 4.1 %, the effect of steel appeared significantly in the RC-columns under the same test conditions. So, the hybrid column had a higher index of ductility than its counterpart reinforced with full steel because of the large core of the hybrid, which gives it a higher resistance. It is also higher than its counterpart reinforced with full GFRP, as the steel has a higher modulus of elasticity.

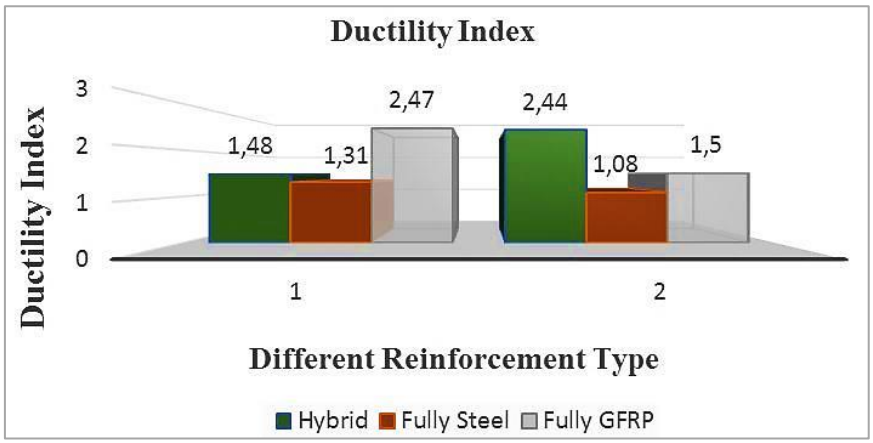

Fig. 15: Ductility index for different reinforcement types: 1 - ρ 1.6 %, 2 - ρ 4.1 %.

Conclusions

1) All column failures were attributable to concrete crushing under compression control depending on the reinforcement ratio and the transverse reinforcing type or spacing.

2) Increasing the longitudinal reinforcement ratio from 1.6 % to 4.1 % marginalizes the load carrying capacity of GFRP-RC columns subjected to concentric loading. In comparison, it significantly affects columns exposed to eccentric loading by increasing the ultimate capacity by 83.5 and 177.4 % for columns with tie spacing of 60 mm and e/h = 0.21 and 0.42, respectively. Also, by 48.7 and 62.7 % for columns with 120 mm tie spacing.

3) A slight increase in the carrying capacity of columns at 60 mm spacing between ties compared to spacing of 120 mm under the concentric loading and e/h = 0.42. Whereas, the increment ratio is found to be 3.6 % and 3.2 % for reinforcement ratio of 1.6 % and 4.1 %, respectively for columns which subjected to concentric loading and 5.97 % and 80.73 % of reinforcement ratios 1.6 % and 4.1 % respectively for columns with e/h = 0.42. On the other hand, the increment ratio of carrying capacity of columns with e/h = 0.21 are found to be 40.71 % and 14 % for reinforcement ratios of 1.6 % and 4.1 %, respectively.

4) For concentric loading the columns with the highest reinforcement ratio have the highest strain. Whereas in the case of eccentric loading 30 and 60 mm, it was found that the columns with the lowest reinforcement ratio had the highest amount of strain.

5) In concentric loading columns, reducing the spacing between ties enhances the resistance of columns. Accordingly, the strain in the stirrups increases due to the applied load. In contrast, in the eccentrically loaded column, the increased spacing between ties increases the bearing capacity of the column, so the transverse reinforcement strain rises due to the applied load.

6) Columns under concentric loading confined with GFRP ties at 60 mm spacing between ties for 1.6 % and 4.1 % reinforcement ratio showed higher bar strength contribution than their counterpart confined with 120 mm spacing between ties.

7) The lateral and vertical displacement amount is reduced in columns with a higher reinforcement ratio than their counterparts with a lower reinforcement ratio.

8) Reducing the spacing between ties when applying concentric load on the specimens provides high confinement of the core thus, the lateral displacement is reduced. But the opposite result was observed when the column was subjected to a 30 mm eccentricity applied load. As for the

high eccentricity, found reverse behavior of 30 mm eccentric loading the lateral displacement increase with increases tie spacing causes higher load carrying capacities.

9) It found that columns reinforcing with fully GFRP have the highest vertical displacement because of their lowest bearing capacity.

10) For full GFRP RC-columns, it is evident that the ductility index of columns with 60 mm tie spacing decreased as the eccentricity increased. On the other hand, the ductility index values of columns of 120 mm tie spacing decrease when e/h is equal to 0.21 and then increase when *e*/*h* reaches 0.42.

11) Reducing the spacing of 60 mm for columns reinforced with fully GFRP exhibited higher ductility than their counterpart which fully steel reinforced columns at 120 mm spacing between ties, this finding indicates that utilizing GFRP in reinforcing concrete columns by reducing confined spacing gives credit for GFRP to achieve the desired purpose of replacing steel, which is one of the aims of the current study.

12) The test results indicate that at the minimal reinforcement ratio 1.6 %, the steel effectiveness did not manifest in the columns' ductility. In contrast, for a higher reinforcement ratio 4.1 %, the effect of steel appeared significantly in the RC-columns. Besides, the hybrid column had a higher index of ductility than its counterpart reinforced with full steel and full GFRP.

References

[1] GAMBLE, W. L.: Eccentric Behavior of Full-Scale Reinforced Concrete Columns with Glass Fiber-Reinforced Polymer Bars and Ties. ACI Structural Journal, Vol. 116, Iss. 1, 2019, pp. 275-277.
[2] AMERICAN CONCRETE INSTITUTE ACI Committee. Building Code Requirements for Structural Concrete ACI 318-19 and Commentary 318R–19. American Concrete Institute ACI Committee, 2019.
[3] ABDELAZIM, W. et al.: Proposed slenderness limit for glass fiber-reinforced polymer-reinforced concrete columns based on experiments and buckling analysis. ACI Structural Journal, Vol. 117, Iss. 1, 2020, pp. 241-254.
[4] GUÉRIN, M. et al.: Eccentric Behavior of Full-Scale Reinforced Concrete Columns with Glass Fiber-Reinforced Polymer Bars and Ties. ACI Structural Journal, Vol. 115, Iss. 2, 2018, pp. 489-499.
[5] SALAH-ELDIN, A. - MOHAMED, H. M. - BENMOKRANE, B.: Structural performance of high-strength-concrete columns reinforced with GFRP bars and ties subjected to eccentric loads. Engineering Structures, Vol. 185, 2019, pp. 286-300.
[6] JIANG, T. - TENG, J. G.: Behavior and design of slender FRP-confined circular RC columns. Journal of Composites for Construction, Vol. 17, Iss. 4, 2013, pp. 443-453.
[7] ACI COMMITTEE 440. Guide for The Design and Construction of Concrete Reinforced with FRP Bars, ACI 440.1R-15. American Concrete Institute ACI Committee, 2015.
[8] ISSA, M. - METWALLY, I. - ELZEINY, S.: Performance of eccentrically loaded GFRP reinforced concrete columns. World Journal of Engineering, Vol. 9, No. 1, 2012, pp. 71-78.
[9] KHORRAMIAN, K. - SADEGHIAN, P.: Behavior of slender GFRP reinforced concrete columns. ASCE-SEI structures congress. American Society of Civil Engineers, 2019.
[10] KHORRAMIAN, K. - SADEGHIAN, P.: Experimental and analytical behavior of short concrete columns reinforced with GFRP bars under eccentric loading. Engineering structures, Vol. 151, 2017, pp. 761-773.
[11] HADHOOD, A. et al.: Efficiency of glass-fiber reinforced-polymer (GFRP) discrete hoops and bars in concrete columns under combined axial and flexural loads. Composites Part B: Engineering, Vol. 114, 2017, pp. 223-236.
[12] HADHOOD, A. - MOHAMED, H. M. - BENMOKRANE, B.: Axial load–moment interaction diagram of circular concrete columns reinforced with CFRP bars and spirals: Experimental and theoretical investigations. Journal of Composites for Construction, Vol. 21, Iss. 2, 2017, 12 p.
[13] TOBBI, H. - FARGHALY, A. S. - BENMOKRANE, B.: Behavior of Concentrically Loaded Fiber-Reinforced Polymer Reinforced Concrete Columns with Varying Reinforcement Types and Ratios. ACI Structural Journal, Vol. 111, Iss. 2, 2014.
[14] ALWASH, N. A. - JASIM, A. H.: Behavior of short concrete columns reinforced by CFRP bars and subjected to eccentric load. Technology, Vol. 6, Iss.10, 2015, pp. 15-24.
[15] OTHMAN, Z. S. - MOHAMMAD, A. H.: Behavior of eccentric concrete columns reinforced with carbon fiber-reinforced polymer bars. Advances in civil engineering, Vol. 2019, 2019.
[16] EL-GAMAL, S. - ALSHAREEDAH, O.: Behavior of axially loaded low-strength concrete columns reinforced with GFRP bars and spirals. Engineering Structures, Vol. 216, 2020, 15 p.

[17] AL-HELFI, M. - ALLAMI, A.: Experimental Work to Study the Strengthening Effect of SFR and CFRP on a Part or Whole of the Length of Slender RC Columns. Civil and Environmental Engineering, Vol. 17, Iss. 1, 2021, pp. 9-22.
[18] ASTM INTERNATIONAL Standard Test Method for Compressive Strength of Cylindrical Concrete Specimens. ASTM International. ASTM C39/C39M-17, West Conshohocken, PA 2017.
[19] ASTM INTERNATIONAL Standard Test Method for Tensile Properties of Fiber Reinforced Polymer Matrix Composite Bars. ASTM D7205/D7205M-06, West Conshohocken, PA 2016.
[20] PESSIKI, S. - PIERONI, A.: Axial load behavior of largescale spirally reinforced high-strength concrete columns. Structural Journal, Vol. 94, Iss. 3, 1997, pp. 304-314.
[21] ELMESSALAMI, N. - ABED, F. - EL REFAI, A.: Response of concrete columns reinforced with longitudinal and transverse BFRP bars under concentric and eccentric loading. Composite Structures, Vol. 255, 2021, 12 p.